THE FUTURE OF LOW SPEED SCRUBBING TECHNOLOGY

Alexander Michael Brown

Department of Chemical Engineering, University of California, Berkeley, CA, USA.

Abstract: Low Speed Scrubbing Technology (LSST) is a new technology for the purification of industrial exhausts from both gaseous and solid pollutants. It does not belong to either a counter-flow or co-flow system, but is based on the idea of regime change. The LSST scrubber, known as the Low Speed Absorber (LSA), is free of any mechanical or pressure loads, has low hydraulic resistance, and has no unreliable structural units. It is a foolproof and serviceable construction.

Keywords: Low Speed Scrubbing Technology (LSST), Low Speed Absorber (LSA), gas-liquid interaction, sorption, chemisorption, wet scrubber, absorber, counter-flow, co-flow, regime change

Introduction

Non-catalytic sorption/chemisorptions as a whole, including gas-liquid interaction in particular, is conceptually a phenomenon of a physico-chemical nature. It consists of the physical process of gas dilution in the liquid phase followed by a chemical interaction. These processes are well understood[1-5]. Theory and design principles permit rate (efficiency) and limits of the sorption depending on both physico-chemical parameters of the process and engineering design to be quickly and reliably estimated. In engineering, these processes are usually done in units known as wet-scrubbers (or absorbers), the scrubbing process (i.e., gas/liquid interaction) proceeding as either a counter-flow or co-flow regime. In addition to the conventional co/counter-flow technologies, Low Speed Scrubbing Technology (LSST) is intended for the purification of industrial exhausts from both gaseous and solid (dust) pollutants[6,7]. It does not belong to either a counter-flow or co-flow system, but is based on the idea of regime change[8-12]. For practical embodiment, a scrubber of special design known as Low Speed Absorber (LSA) is required. To gain an insight into both the theoretical basis and to design features of this technology, it is useful to follow a process in the simplest one-stage LSA.

General description

One-stage LSA conceptually consists of the contacting chamber, separation chamber, fixed (immovable) centrifugal separator, and various hydraulic units (Fig. 1) and functions as follows.

The initial contaminated gas enters the contacting chamber from the bottom upward and starts to ascend. At this stage it meets a liquid jet descending via back-pipes from the separation chamber joined from above. Initially, the discharge liquid jet is compact. Then it simultaneously starts to fall under gravity and break down into smaller fragments (regular and irregular drops) on exposure to the ascending gas. As this takes place, the small drops (i.e., with weights smaller than the dynamic pressure of the ascending gas) are instantly picked up by the ascending gas and start to ascend jointly with the gas. The heavier drops continue to descent and split concurrently, thus regenerating both small and large drops. Eventually, spontaneous self-fragmentation terminates. Aerosols result from this process and continue to fall until retarding forces become initially equal to gravity and then more than gravity for any liquid fragment. From this point on, the dispersed liquid phase starts to ascend.
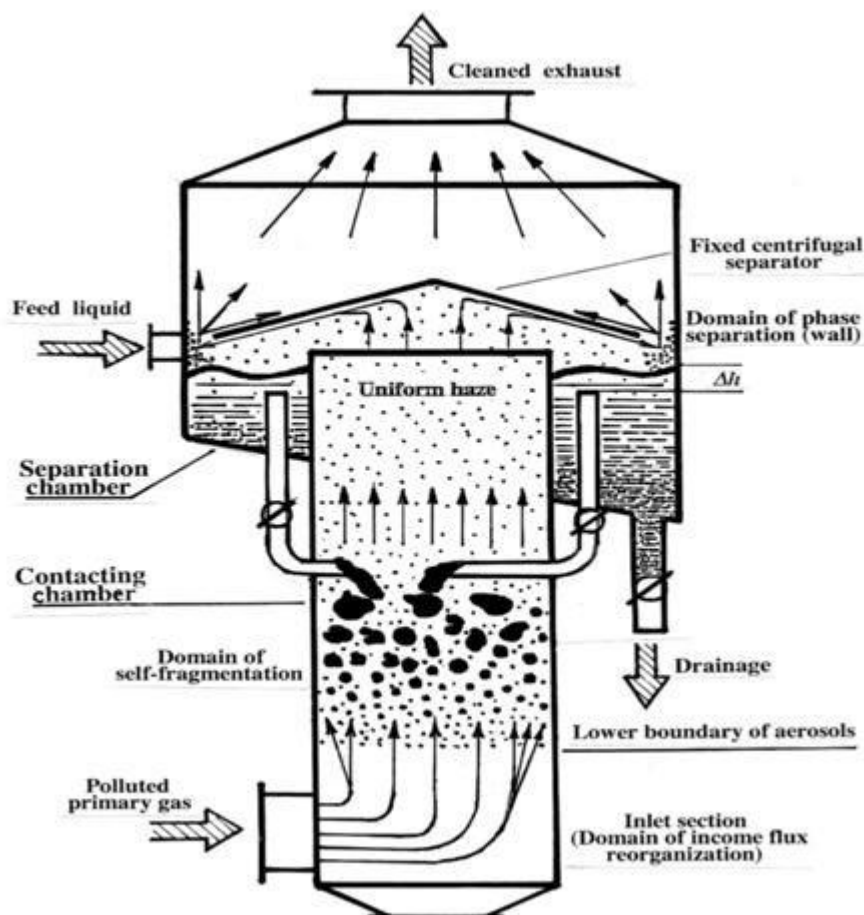
Figure. 1. Schematic diagram of one-stage Low Speed Absorber (LSA).

This aerosol leaves the contacting chamber and enters the fixed centrifugal separator of the separation chamber located above. Welded curvilinear blades of the fixed centrifugal separator direct haze onto the wall of the separation chamber. Here actual phase separation occurs: the gas exits into the atmosphere as the cleaned exhaust, while the liquid flows down the wall and accumulates at the bottom of the separation chamber. Then the densest portion (i.e., lower layers of the liquid) is drained via a drainage outlet, while the most aerated portion (i.e., upper layers) is partially recycled under gravity via back-pipes to the contacting chamber. In this way, there is an inner automatic recycling of the liquid phase between the contacting and separation chambers. Its special feature lies in the fact that the times of phase contact relative to gas and liquid are dependent on different factors and hence can be controlled independently. Contact time on the gas side is completely predetermined by the gas speed, while contact time on the liquid side depends on the gas speed and the regime of liquid phase renewal (i.e. ratio of the feed and drained liquid fluxes). The latter, in turn, is a function of the current physico-chemical properties of the liquid and dispatch state. Contact time on the liquid side is evidently unlimited and should be set accordingly to the efficiency of mass exchange by means of the variation of liquid phase renewal. Hence, control valves of feed liquid and drainage can vary the contact time from the liquid side independently and simply. By and large, this provides high flexibility of the practical control of LSA operation.

A point of any scrubbing technology is to mix the gas and liquid phases as well as possible. Diverse conventional devices (e.g., packings, mechanical agitators, or mixers, as well as injectors, nozzles, etc.) are designed for suitable solution of the mixing problem. LSST has no need for any man-made mixing device because it is the counteraction between inertia forces of the ascending gas and the gravity forces of the descending liquid that triggers self-fragmentation and acts as a natural stirrer. This "stirrer" is uniformly distributed over the whole volume; it affects all spatial points of the contacting chamber. Therefore, the back-pipes connecting the separation and contacting chambers are standard tubes rather than some specific injectors. The mode of operation (continuous, periodical, etc.) of drainage and supply of feed liquid, as well as the amount of the recycling liquid, is dictated by both sorption features and liquid properties. It facilitates easy remote control through the control valves. In this way, the low speed scrubbing process begins as a counter-flow while it terminates as a co-flow.

Theoretical fundamentals

The most general equation of unsteady heat/mass exchange between the gas and dispersed liquid phase is of the form [1]

$$\frac{\partial c}{\partial \tau} = \frac{1}{Ped}\frac{\partial^2 c}{\partial \xi^2} - \frac{1}{\sqrt{g_s}}\frac{\partial(c,\psi)}{\partial(\xi,\eta)} \qquad (1)$$

ξ,η are dimensionless co-ordinates, $g_s=\{g^{11},g^{12},g^{22}\}\neq 0$ is the metric tensor. Leaving aside Here , , any details of formal transformation, Eq. (1) can be eventually reduced[1,13,14] to the well-known equation of unsteady diffusion as follows:

$$\frac{\partial c}{\partial \tau} = \frac{\partial}{\partial x}\left(d\frac{\partial c}{\partial x}\right) \qquad (2)$$

The solution of Eq. (2) depends on the nature of transfer processes, reciprocity of transfer phenomena and chemical processes, as well as initial and boundary conditions. In the approximation of the diffusion boundary layer, these items are usually considered with the help of similarity criteria in the following way:

$$Nu_d = F\,(Re,\, Pe_d,\, Sc,\, Fr) \qquad (3)$$

$$Re = \frac{Lu}{\nu}, \quad Pe_d = \frac{Lu}{d}, \quad Pr_d(Sc) = \frac{\nu}{d}, \quad Fr = \frac{u^2}{gL}$$

Physically, these determining criteria consider the nature of gas flow (Reynolds number Re), the interdependence of convection and diffusion transfer (Peclet number Pe_d), the similarity of the speed and concentration fields (either Schmidt number Sc or Prandtl number for diffusion Pr_d), and scale factor (Froude number Fr). The most comprehensive theoretical analysis of various specific cases (e.g., Stokes regime/potential flow, laminar/turbulent motion, small/large Pe-criteria, surface/volume chemical reaction) can be found in Gupalo et al [6]. Practical use of similarity theory requires knowledge of both hydro/gas-dynamics essentials and numerical values of parameters as initial and boundary conditions (i.e., design features). The former can be revealed by pure analysis, while the latter are only experimentally determined.

Hydro/gas-dynamics

As can be seen from above, LSST possesses specific hydro/gas-dynamics. Compared to conventional co/counter-flow systems, the essentials of LSST hydro/gas-dynamics can be explained as follows. To provide a stable LSST

regime, the counteraction between inertial forces of the ascending gas and gravity forces F_N of the descending liquid takes place under prevalence of the former relative to the drop of any R-size. The fall rate of the very large drops $R_\square > R > R_{sf}$ (compact liquid jet $R_\square$ and the boundary of self-fragmentation R_{sf} are the limits) is independent of the drop weight and size while solely is dependent on gravity

$$F_N \sim (mg)_l \sim (4/3)\square\square g R^3 \tag{4}$$

At the same time, the fall rate of the smaller drops $R < R_{sf}$ is essentially dependent on their size. Any R-drop maintains its integrity until consolidating forces (surface tension F_s)

$$F_s \sim \square R \tag{5}$$ exceed

breaking forces of resistance to the motion, the latter being a function of the motion regime and size of drop Re

$$\square \quad \square u L \quad \square \quad \square\square \quad \square \quad \mathrm{Re}_{cr} \quad \square \quad \text{laminar flow} \tag{6}$$

$$\square \quad _\square \quad \square \quad \mathrm{Re}_{cr} \quad \square \quad \text{turbulent flow}$$

For the turbulent flow around a small sphere $R \sim 10^{-6}$ m, local $Re_{cr} \sim 10$, while resistance forces F_t are proportional to the drag force of the gas and the drop size

$$F_t \sim (\square u^2)_{gas} R^2 \tag{7}$$

The comparison of F_s and F_t (Eq. 5, 7) shows that the upper limit of fragmentation is non-existent, i.e., the breaking forces prevail over the consolidating ones under all conditions, including the limit $R_\square$ of compact liquid jet. Physically, this means that any free-falling compact liquid jet disintegrates inevitably sooner or later. Spontaneous self-fragmentation terminates at the point when the velocity head of the ascending gas becomes equal to the forces that determine both the scale and integrity of the drop (i.e., surface tension). Thus, the lower limit of selffragmentation is dictated by their equality $F_s \sim F_t$

$$Rsf \square \underline{\quad\quad} \square u2 \square \tag{8}$$

Hence, R_{sf} is dependent on the gas speed. It is easy to see that for pure water ($\square\square 1000$ kg/m^3, $\square_{75} \square$ 65 kg/s^2, $\square_{75}\square 3.8 \cdot 10^{-4}$ kg/m·s) and typical LSST regimes $u \sim (10-20)$ m/s, the average size distribution lies mainly within the range $R_{sf} \sim (100-500) \cdot 10^{-6}$ m. Redistribution of size grading in the domain located below the level of the backpipes is governed by the scrubbing speed and properties of the liquid phase. Specifically, the surviving drops $R_{sf} > R > R_1$ maintain their integrity and continue to fall in the turbulent regime as long as the condition $Re > Re_{cr}$ of Eq. (6) remains valid. Finer drops $R_1 > R > R_2$ fit the condition $Re < Re_{cr}$ of Eq. (6) and fall in the laminar regime. They are exposed to the breaking forces of the conventional gas-dynamic (Stokes) nature

$$6\square Ru\square \underline{\quad\quad\quad} \square 6\square Ru\square$$
$$(1\square\square/R)$$

$$F_{St} = \tag{9}$$

As follows from Eq. (4, 9), limiting R_1-values fall in the range $R_1 \sim (50-100) \cdot 10^{-6}$ m for typical LSST gas speeds $u \sim (10-20)$ m/s. Finally, the finest drops $R < R_2$ maintain their integrity while never falling. Once generated, they are immediately carried by the ascending gas into the separation chamber. The main feature of their motion lies in the fact that their absolute velocity is equal to the velocity of the gas carrier. In other words, the relative velocity of their motion equals zero. Thus, collisions rarely occur and this finest fraction survives up to the final exhaust (unless special measures are implemented).

The upper limit R_2 is dependent on scale height of the medium $H=kT/mg$ and for the limiting case of free fall, it can be estimated as

$$^2 \square 1/7$$
$$\square \, kT \square$$

$$\square \underline{\qquad} \square$$
$$R_2 \square \, \square^\square \square 3l \, g2 \, \square\square \, \square \, 10\text{-}6 \text{ m.}$$

Thus, the hydro/gas-dynamic pattern of disintegration can be generalized as follows:

$R_\square > R > R_{sf}$ -free (Newton) fall, progressive self-fragmentation, settling rate is independent of drop size,

$R_{sf} > R > R_1$ - turbulent motion, partial fragmentation of the coarsest portion of aerosols is admissible, settling rate depends on drop size as $u \sim R^{1/2}$,

$R_1 > R > R_2$ - laminar (Stokes) motion, no fragmentation, settling rate depends on drop size as $u \sim R^2$,

$R_2 > R$ - forced ascent (no fall), neither fragmentation nor drop growth occurs.

The zone of self-fragmentation (domain between the level of the back-pipes and lower spatial boundary of aerosol) contains a very wide spectrum of drops $R_2 < R < R_\square$. At the same time, the domain located above the level of the back-pipes contains finer aerosol $R_2 < R < R_{sf}$ (thin haze), i.e., this zone is far more uniform in the sense of size distribution.

So far only destruction has been considered. Various transfer effects (e.g., gravity, diffusion, convection) lead to collisions followed by coagulation of drops resulting in their growth [15]. Physically, the upper limit of this growth is evident, since any newly formed drop R_{new} to be smaller than the limiting values R_{sf}, R_1, R_2 along the whole associated range of physical conditions. Otherwise, if such drop $R_{new} > R_{sf}$, R_1, R_2 is generated, then it will be destroyed again.

The growth of any drop $R(\square)$ along the fall distance $dZ=ud\square$ depends on both number of collisions and liquid-water content G_l kg/m^3. For free fall, the relation between current mass dm of some R-drop and motion parameters

$$2\square g \square lR^4 \, G_l \underline{\qquad}$$
$$^2 dR \sim G_l \square R^2 dZ \sim G_l \square R^2 ud\square \, \sim \quad 9\square \, d\square \qquad (10) \qquad dm \sim (4/3)\square \square_{ini} R$$

allows for simple estimation of both dynamics of drop growth (terms 2 and 3)

$$\sim \qquad \frac{dR}{dZ} \, \frac{G_l}{4^{\square l}} \qquad (11)$$

and fall time considers this growth (terms 2 and 5 of Eq. (10))

$$18\square$$
$$\overline{\qquad}$$
$$gG^l R^{ini} \qquad (12) \qquad \square_f$$

Eq. (11) shows that the drop growth is independent of the motion regime, while Eq. (12) demonstrates that the fall time is independent of the final drop size (since the latter does not appear in Eq. (12)), being dependent only on the initial size R_{ini}. Eventually, the gravity force acting on any drop becomes less than the force of tractive resistance resulting in the termination of the fall.

From this point on, the ascending gas selects and includes all liquid drops. The bottom spatial boundary of the fall distance represents the separation line between the domain of the incoming gas and the self-fragmentation zone, while the top boundary (i.e., back-pipes level) is the separation line between the self-fragmentation zone and the fine aerosols. Above the level of the back-pipes, any small object $R_2 \square R \square R_{sf}$ (no matter whether liquid or solid) acquires the velocity of the gas carrier.

Thus, the consideration of coagulation has a marginal effect on the general pattern. At the same time, it is relevant in relation to the current value of the interfacial area and intensity of heat/mass exchange between the gas carrier and the dispersed liquid phase. The collision of drops results in size redistribution during counter-way traffic of large (falling) drops and small (ascending) droplets, i.e., along the entire length of fall distance Z. Interaction of the ascending and descending dispersed objects is extremely favourable. In gas dynamics terms[15], it increases residence time $\square_{life}$. But more significantly, it enforces the sorption because of the continuous renewal of the interfacial area. Both of these factors considerably improve the mass exchange coefficient $\square$, the latter being the most important generalised index of the sorption efficiency[4,13,16].

As is evident, self-fragmentation time, fall time, residence time and fall distance lie in averaged ranges $\square_{sf} \sim [(2/10^4)\square_l R_{ini} R_f)]^{1/2} \sim (0.05\text{-}0.20)$ s, $\square_f \sim (0.3\text{-}1.0)$ s, $\square_{life} \sim (1.0\text{-}2.5)$ s and $Z \sim (0.5\text{-}1.2)$ m, respectively. The specific interfacial surface S is the interfacial area per unit volume [m^2/m^3]. It is one of the most important indices among others. With the assumptions of normal (Gauss) size distribution and spherical shape of the drops, it can be approximated as $S \sim 3 \cdot 10^3/R \sim (400\text{-}800)$ m^2/m^3 depending on gas speed $u \sim (10\text{-}20)$ m/s and volumetric flux of water $\square \sim (0.02\text{-}0.10)$ $m^3/m^2 s$. These estimates are in good agreement with the direct experimental data [17] (Fig. 2).
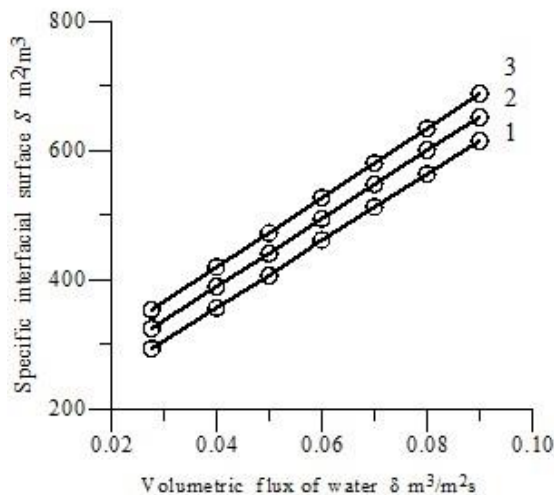

Figure. 2. Specific interfacial surface S versus volumetric flux of water $\square$. 1- u= 10 m/s, 2- u= 15 m/s, 3-u= 20 m/s.

To generalise, it should be stated that in deciding on scrubbing speed, the dominance of gas momentum over liquid momentum

$$(\square u)_g > (\square u)_l \qquad (13)$$

is the single crucial constraint of LSST applicability.

Experiment

To suit the similarity theory, the experimental apparatus for LSST investigation was designed as a transparent 1:10 reduced scale model of a typical cylinder-shape full-scale scrubber of 50000 nm^3/h gas load (Fig. 1). Values of the main criteria $Re_{model}= Re_{nature}$, $Pe_{d, model}=Pe_{d, nature}$, $Sc_{model}=Sc_{nature}$ were satisfied. Other criteria, including Fr and thermal, were held constant whenever possible. Measurements of the contacting and separation chambers were equal to D=0.4 m, L=1.1 m and D=1.0 m, L=0.7 m, respectively. Total gas load, gas spead and volumetric flux of water varied within the limits V_g~(1.0-3.0) m^3/s, u~(8-25) m/s, and □~(0.02-0.10) m^3/m^2s, respectively. Polluted primary gas contains various admixtures (e.g., phenol, ammonia, hydrochloric acid). Below are given data regarding primary gas polluted with the mixture {(2-8)% SO_2+(1-4)%SO_3}. With the control system, high-speed (up to 5000 shots/s) photography and on-line measurement of the main process characteristics were possible. Other details can be found elsewhere [10,17, 18].

The prime object lies in the direct experimental determination of the main technological (residence time, fall time and distance, interfacial area, size distribution and zoning of the dispersed phase) and sorption indices (heat/mass-exchange coefficients □), which are dependent on LSST operating parameters (gas load, scrubbing rate and volumetric flux of water) and LSA design features (geometric and aspect ratios, positional relationship of various units and hydraulic resistance). Experimental data combined with the essentials of dimensional analysis provide adequate LSST description to yield simple analytical quantities for practical LSA design. Relevant data[17,18] are shown in Figures 2-4 and Table 1 and can be briefly summarized.

Table 1. The main LSST and LSA scrubbing variables

	Indices	Wet-bed	Venturi tube	One-stage LSA
1	Gas load (*max*), V_g nm^3/h	~180 000	<100 000	300 000
2	Number of stages in one set	1-2	1	Any
3	Operational regime	Co/counter	Only co-flow	Compound
4	Interfacial area, S m^2/m^3	*max* 250	*max* 400	400-800
5	Gas speed, u m/s	20-40	50-120	10-20
6	Contact time, □ s	0.05-0.30	0.02-0.10	0.20-2.50
7	Volumetric flux of water □ m^3/m^2s	0.04-0.10	0.40-1.10	0.02-0.10
8	Hydraulic resistance H, Pa	2000-2500	3000-8000	<1400
9	Coefficient of the gas mass exchange □$_{v,g}$ m^3/m^3s	5-8	7-12	20-30 (see text)
10	Cleaning efficiency[*](dust)%	<85	<95	>98
11	Cleaning efficiency (oxides)	~(50-90)%	~(60-95)%	~(70-99)%
12	Dimensions (averaged), m	~ 5.0 / 10.0	~ 3.0 / 6.0	~ 3.5/10.0

| 13 | Dry mass (averaged), *kg* | ~ 10000 | ~ 6000 | ~ 9000 |

Notes : * Strongly depends on size distribution R=R(u).

Specific interfacial surface *S* was determined experimentally by a known chemical method[19]. *S* is almost independent of the gas speed, while it is strongly dependent on volumetric flux of water (Fig. 2). This dependence can be approximated with an accuracy of 12% in the form

$$S \square 1775 \square u^{0.2 \square 0.63}$$ (14)

Fig. 2 and Eq. (14) conceptually confirm the validity of the above presented theoretical approximation. At the same time, the weakened *S-u* correlation seems to be the result of some liquid loss from the contacting chamber as the gas speed increases.

Both mass holdup of liquid g_l kg

$$g_l = G_l/V = ^{0.209 \square u \square 0.79 \square 0.92}$$ (15)

and its residence time $\square_{life}$ in the contacting chamber

$$\square_{life} = L_{cont}/ \square$$ (16) are strongly dependent on volumetric flux of water $\square$. The volumetric holdup of gas in the contacting chamber v_g is defined as the difference between the volume of contacting chamber *V* and volumetric holdup of liquid $v_l = g_l/\square_l$

$$v_g = V - v_l$$ (17)

Usually, volumetric fraction of gas $\square_g = v_g/v_l$ falls in the range (0.90-0.98). The main interest was focused on the direct experimental determination of mass exchange efficiency and search for opportunity of its intensification in the context of the unsteady phase interaction. Some of the generalised results are briefly summarized as follows.

Mass-exchange efficiency of LSST was estimated with the help of the following transfer coefficients. The coefficient of the liquid mass exchange $\square_{v,l}$ represents volumetric gas flux from the gas phase to the liquid phase with respect to the whole gas-liquid volume. It was determined experimentally by the example of carbon dioxide CO_2 desorption from its aqueous solution. $\square_{v,l}$-values are dependent on the gas speed and volumetric flux of water (Fig. 3); the semi-empirical average approximation is in the form

$$\square_{v,l} = ^{0.457 \square u 0.25 \square 0.86}$$ (18) with an accuracy of 10%.

A comparison of Eq. (14) and (18) shows that the gas speed affects both $\square_{v,l}$ and *S* equally. As a result, the coefficient of the surface mass exchange $\square_{v,S}$, i.e., volumetric gas flux from the gas phase to the liquid phase with reference to the specific interfacial surface *S,* seems to be practically independent of the gas speed. Both the direct experimental plot of $\square_{v,S}$ vs *u* (Fig. 3) and semi-empirical analytic approximation

$$\square_{v,S} = \square_{v,l}/S = 0.0003 ^{u0.05 \square 0.23}$$ (19) prove this feature of mass exchange in LSA.
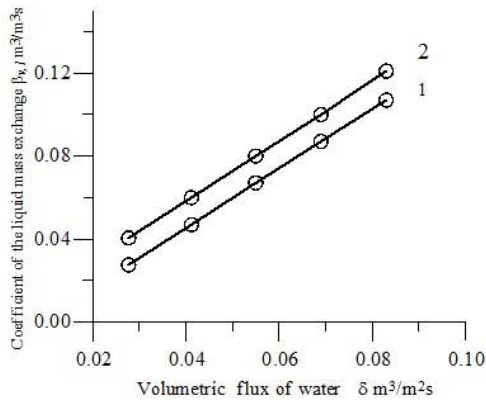
Fig. 3. Coefficient of the liquid mass exchange $\square_{v,l}$ versus volumetric flux of water $\square$, 1- u= 10 m/s, 2-u= 20 m/s.

The coefficient of the gas mass exchange $\square_{v,g}$, i.e., volumetric gas flux from the gas phase to the liquid phase with reference to the gas volume, was determined experimentally through the rate of adiabatic evaporation of water. The weaker the solution, the more valid the method [20]. Therefore its use is justified considering that the solution strength does not exceed ~ 20%. The correlation of $\square_{v,g}$ with the length of the conacting chamber for a different gas speed u and volumetric flux of water $\square$ is displayed in Fig. 4. The coefficient of the gas mass exchange $\square_{v,g}$ represents (by definition) the average product of some local index $(\square_{v,g})_{loc}$ and local interfacial surface S_{loc}. Therefore, its decrease along the contacting chamber length is attributed to the decrease of either $(\square_{v,g})_{loc}$ or S_{loc}. The former could occur if the diffusion on the gas side through the boundary layer quickly decays for any reason (e.g., fast equalisation of phase potentials). Otherwise, the governing factor is the duration of boundary layer formation. As to the possible decrease of S_{loc}, it may occur due to either coagulation (see above) or the effect of initial and boundary conditions.

Any other admissible reason for $\square_{v,g}$ variation is dismissed because of the high values of Re and Pe-criteria (Re~ 10^5, i.e., it is turbulent regime, while Pe~ 10^3, i.e., convection is the dominant process). The elbow (saturation) of the curve in Fig. 4 marks the termination of the transitional unsteady period of two-phase flow formation and transition to the steady flow regime.
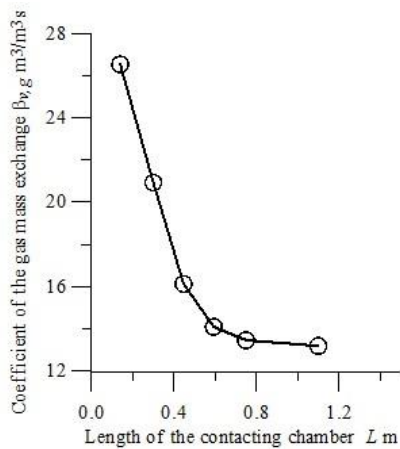

Fig. 4. Coefficient of the gas mass exchange $\square_{v,g}$ versus height of the contacting chamber L$_{cont}$.

A specific feature of the transfer coefficient $\square$ lies in the fact that it is the most generalised index of scrubbing efficiency and hence it is a function of both the operating conditions $\square=\square$ (P, T, u, $\square$) and design features $\square=\square$

(L, D, $\square$, S). However, the former is more or less restricted and cannot be widely varied, while the latter is completely dependent on hydro/gas-dynamics. This means that the mass exchange can be restrictively varied only by optimisation of the LSA design. Thus, from the specific point of view of the LSA designer, data in Fig. 4 should be read as a practical recommendation for initial approximation of the contacting chamber dimensions. Depending on the given flow sheet and customer's demands, this quantity will be specified later in the project development. The achieved values of index $\square$ can be found in Figures 3 and 4 and Table 1. The simplified entry of the overall purification efficiency can be presented in the form[5]:

$$\square G \sim \square \cdot \square \; \square \; S \qquad (20)$$

Here $\square G$ is total amount of captured and fixed impurity (whether it be gas, liquid or solid), $\square$ is volumetric flux of liquid, $\square$ is residence time, S is specific interfacial surface, while $\square$ represents mass exchange coefficient. The average values of these quantities for LSST typical regimes fall within the following ranges. Volumetric flux of water is predetermined by gas momentum $(\square u)_g$ and lies in the range $\square \sim (0.02\text{-}0.10)$ m^3/m^{2}s. The residence time is the sum of the fall time and one of the ascending co-flow along the contacting chamber $\square_l = L/u$, being equal to $\square_{life} = \square_f + \square_l \sim (0.2\text{-}2.5)$ s. It should be stressed that increase of the gas speed from u_1 to $u_2 = nu_1$, $n>1$ implies not only the growth of the interfacial area, but also quadratic increase in the hydraulic resistance $\square H = H_2/H_1 \sim \square (u_2)^2 / \square (u_1)^2 \sim \square (nu_1)^2 / \square (u_1)^2 \; \square n^2$, enforced carrying away of the dispersed phase from the contacting chamber and non-linear decrease of contact time $\square \sim (\square u)^{-1}$. In doing so, the product $(S\square)$ is correlated in such a way that it is a non-monotonous extremal function. Location of its extremum is dependent on the sorption efficiency and cannot be estimated *a priori*.

Design and engineering features

LSA units must provide both the main and some subsidiary technological operations. The inlet section is the domain of the incoming gas flux reorganization (Fig. 1). It is designed for gas input and (should the need arise) the cooling of the gas by water injection. These operations can be separated; however, the combined design offers definite advantages. A contacting chamber of typical length/diameter ratio $(L/D)_{cont} \sim (1.0\text{-}1.5)$ serves for mixing and sorption, as well as regime stabilisation in cases of wide gas load variation or frequent (spontaneous) input/output operations. For this purpose, it can be arranged with a stabilising circular collar. The latter is installed so as to divide the inlet and contact zones. Usually, this collar is the split ring, the details (shape, number of segments and coefficient of wetted passage $\square = S_{free}/S_{cont}$) being completely determined by the flow sheet. The height of the liquid bulk in the separation chamber h_{level} is usually chosen in such a way as to provide a hydrostatic head on the recycling back-pipes $\square h = h_{level} - h_{pipes} \sim (0.1\text{-}0.3)$ m. In turn, both the overall cross-section of back-pipes $S_{pipes} \sim 0.785 d^2 (\square h)^{1/2} / \square (2g)^{1/2}$ (here $\square = 1.8 \cdot (\square h)^{0.92} \square^{-0.61}$ is the coefficient of liquid discharge) and their total number $m \sim S_{pipes}/0.785 d^2$ are dictated by volumetric flux of water $\square$ and gas speed u. The fixed centrifugal separator also has some special features, particularly the efficiency of phase separation, which is very sensitive with respect to the separator geometry, including number, height, and curvature of curvilinear blades. The dimensions of the separation chamber are dictated primarily by the demands of the total precipitable water (including water vapors and droplets) in the final exhaust, being dependent as well as on the dryness factor of the primary polluted air. For this demand to be fulfilled, the gas speed along the separation chamber $u_{sep} = F(u, R)_{air}$ should be smaller than the deposition rate $u_{air}(R_{air})$ of airborne water droplets of some definite R_{air}-drop. Usually, the ratio $(L/D)_{sep} \sim (0.6\text{-}0.8)$ provides a reasonable solution to this problem. In this case, the ratio between the diameters of the contacting and separation chambers falls in the region $D_{sep}/D_{cont} \sim (u_{cont}/u_{sep})^{1/2} \sim (2\text{-}2.5)$.

In its turn, any LSA can be arranged as a multi-stage unit enclosed in a common shell, any stage in a series being independently optimised along any parameter [9,10]. As this occurs, the next stage is either an identical copy of the preceding stage (so-called cascade LSA) or distinctive in any respect (combined LSA). A cascade LSA is applied for fine cleaning, since the output of the previous stage is simultaneously the input reative to the following one. A combined LSA is used when each taken separately stage is optimized along another parameter.

One remark of material significance

In current engineering practice, the customer's demands are a point in any real design. These demands are usually well known. They include efficiency of purification, minimisation of budget investment and/or operational cost, minimal water consumption, dryness of the exhaust, optimal dimensions, fool-proof design (i.e., safe maintenance achievable with low-skilled operator) and sometimes unforeseen demands. The order of preference (priority) of these demands, together with the given flow sheet, could result not only in simple changes of some details (e.g., dimensions) or even radical ones in design (one, two or three-stage LSA), but often predetermine the possibility of using wet scrubbing technology. Generally, this priority sequence is unpredictable, hence it should be posed and approved *a priori*. Unpredictable priority sequence of customer's demands, specificity of LSST hydro/gas-dynamics, variable combination of physico-chemical parameters, character of the particular industrial site, as well as the very essence of scrubbing, lead to the point that LSA manufacturing is not repetitious work. There are sometimes apparent similarities (e.g., the same scale, impurities, physical conditions and degree of purification), which, in fact, are embodied into drastically different real plants. As is evident, to implement particular LSA, both standard design and intuitive engineering solutions (know-how) need to be used. In other words, each real case is unique and requires its own engineering design [8,10-12].

Discussion and conclusions

Comparison of relevant sorption and technology LSST ability factors with those of some conventional technologies, such as wet-bed[3,5] and Venturi tube techniques[21,22] can be found in Table 1. They show that LSST combines the main merits of conventional co/counter-flow technologies, while being free of their defects.

Two key points that provide the main LSST advantages (primarily high mass-exchange efficiency) are the low absolute gas speed and spontaneous change of the counter-current regime to the co-current one. The decrease of typical gas speeds of conventional co/counter-flow technologies $u\sim(20\text{-}40)$ m/s down to the typical LSST-speeds $u\sim(10\text{-}20)$ m/s does not cause deterioration of the process on the whole; on the contrary, it enhances scrubbing efficiency while reduces control requirements. The main LSST merits and demerits can be generalized as follows. As indicated, both the process as a whole and some of its stages in particular (e.g., mixing, selffragmentation and phase separation) are very sensitive to the LSA geometric proportions. Hence, more sophisticated and careful study of the engineering design (at the stage of the project development) and manufacturing (at the stage of LSA implementation) are necessary. Design errors or inaccurate manufacturing results in dramatic deterioration of scrubbing efficiency. It may be concluded that LSST as a whole presents a successful and effective combination of well-known co-current and counter current technologies. It provides for a stable scrubbing operation and allows for reasonably simple control and monitoring of the latter. The process is conducted by using scrubbers of special design LSA.

Thus, the most specific features of LSA can be summarized as follows:

1.   LSA is free of any (e.g., mechanical and/or pressure) load; hence it is safe in operation.

2.   LSA has no unreliable structural units (e.g., injectors and/or any moving elements) that need careful maintenance; hence a highly skilled operator is not needed. It is a foolproof and serviceable structure.

3.   LSA does not need any auxiliary facilities (e.g., re-circulation pumps).

4. LSA has low hydraulic resistance.

Nomenclature

Design indices

L [m], D [m] and V [m^3] - length, diameter and volume, respectively, *Physico-chemical indices*

$\square$ [kg/m^3] - density,

$\square$ [kg/s^2] - surface tension,

$\square$ [kg/m·s] - dynamic viscosity. *Hydro/gas-dynamic indices*

d [m^2/s] - diffusion constant (Eq. 1, 2), H [Pa] - hydraulic resistance, u [m/s] - speed,

V_g [m^3/s] - total gas load, G_l [kg/m^3] - liquid-water content,

g_l [kg], v_l [m^3] - mass and volumetric holdup of liquid, respectively, g_g [kg], v_g [m^3] - mass and volumetric holdup of gas, respectively,

$\square$ [m^3/m^2·s] - volumetric flux of liquid (current water content)

Heat/mass exchange indices

$\square_{v,g}$ [m^3/m^3·s] - coefficient of the gas mass exchange (volumetric flux from the gas phase to the liquid phase in relation to the gas volume),

$\square_{v,l}$ [m^3/m^3·s] - coefficient of the liquid mass exchange (volumetric flux from the gas phase to the liquid phase in relation to the whole gas-liquid volume),

$\square_{v,S}$ [m^3/m^2·s] - coefficient of the surface mass exchange (volumetric flux from the gas phase to the liquid phase in relation to the specific interfacial surface),

S [m^2/m^3] - specific interfacial surface (interfacial area per unit volume), *Subscripts and abridgements cont* - contact, *f* - fall, *g* - gas, *ini* - initial, *l* - liquid, *loc* - local, *s* - surface, *sep* - separation, *sf* - self-fragmentation.

References

List and codes of air pollutants, 1991, USSR State Department on Environment Protection, Moscow.

Technische Anleitung zur Reinhalyung der Luft (TA Luft), General Administrative Regulation Pertaining the Federal Emission Control Law (Technical instruction on air quality control), 1986, Germany.

Chao, B. T., 1969, Transient heat and mass transfer to a translating droplet, Trans. ASME, Ser. G, J. Heat. Transfer, 91 (2), 273-281.

Levenspiel, O., 1972, Chemical reaction engineering, John Willey and sons, Inc., New York-London-Sydney. Todes, O. M., 1983, Wet-bed absorbers (Rus), Nauka, Leningrad.

Gupalo, Y. P., Polianin, A. D., and Riazantzev Y. S., 1985, Heat/mass-exchange between the flow and reacting particles (Rus), Nauka, Moscow.

Hesketh, K. C., and Howard, E., 1996, Wet scrubbers, Willey, N-Y.

Evgrashenko, V. V., *et al*., 5. 03. 1982, Low-speed foam absorber, USSR a.c. 748940, *ibid.* 12.11.1982, USSR a.c. 839094.

Evgrashenko, V. V., 1983, Design and industrial installation of co-flow scrubber, Ph. D. Thesis, Institute of Chemical Fertilizers and Poisons, Moscow.

Ivanov, V. V., 1988, Fast heat/mass-exchange in LSA, Ph. D. Thesis, Institute of Chemical Fertilizers and Poisons, Moscow.

Dimitrov, V. I., Krainev, G., Evgrashenko, V. V., Slinko, M., and Ivanov, V.V., 8.01.1990, Device for the intensive mass-change, USSR a.c. 1562015.

Dimitrov, V. I., Ivanov, V. V., Krainev, G., and Evgrashenko, V. V., 1992, Low- speed foam absorber, Israel license 102192.

Ruckenstein, E., 1970, Unsteady mass transfer near fluid-liquid interfaces, Chem. Eng. Sci., 25 (11), 1699-1708.

Ruckenstein, E., and Muntean, O., 1970, Mass transfer between a bubble and an oscillating liquid, Chem. Eng. Sci., 25 (7), 1159-1166.

Dimitrov, V. I., and Bar-Nun, A., 1999, A model of energy dependent agglomeration of hydrocarbon aerosol particles, J. of Aer. Sci., 30 (1), 35-49.

Johnson, A. I. Hamielec, A. E., and Haighton, W. T., 1967, Mass transfer with chemical reaction from single gas bubbles, AIChE J., 13 (2), 379-383.

Evgrashenko, V. V., Kernerman, V. A., Ivanov, V. V., Krainev, G., Slinko, M., Holpanov, L. P., and Dimitrov, V. I., 1987, Phase contact in a foam scrubber with the ascending single-pass flow, Chemical Industry, 4, 43-47.

Krainev, G., Evgrashenko, V. V., Slinko, M., Dimitrov, V. I., and Ivanov, V. V., 1987, Estimation of mass-change in two-phase flow, Chemical Industry, 1, 36-38.

Linek, V., and Mayrhoferova, J., 1969, The chemical method for the determination of the interfacial area, Chem. Eng. Sci., 24 (3), 481-496.

Calderbank, P. H. 1959, Mass-exchange in water and aqueous solution of two-phase systems, Trans. Inst. Chem. Eng., v37, N3, 173-184.

Vatanuk, W., 1981, Estimating size and cost of Venture scrubbers, Chemical Engineering, November 30, 93-96. Ollero, P., 1984, Program calculates Venture-scrubber efficiency, Chemical Engineering, May 28, 103-105.